

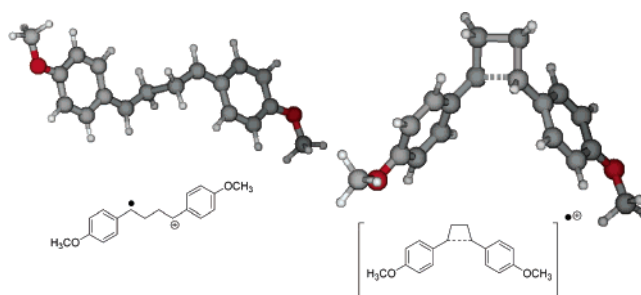
Acyclic or Long-Bond Intermediate in the Electron-Transfer-Catalyzed Dimerization of 4-Methoxystyrene

Lauren L. O'Neil and Olaf Wiest*

Department of Chemistry and Biochemistry, University of Notre Dame, Notre Dame, Indiana 46556-5670

owiest@nd.edu

Received August 23, 2006



The electron-transfer-catalyzed dimerization of 4-methoxystyrene has long been a prototypical reaction for the study of radical cation reactivity. The different possible pathways were explored at the B3LYP/6-31G* level of theory. Both [2 + 2] and [4 + 2] cycloadditions proceed via a stepwise pathway, diverging at an acyclic intermediate and interconnected by a vinylcyclobutane-type rearrangement. The experimentally observed stereoselectivity of the cycloaddition was traced to relatively high barriers for isomerization, while the previously described “long-bond” intermediate could not be located at the higher level of theory. CPCM calculations show that the highly exothermic [4 + 2] pathway becomes kinetically more favorable in condensed phase. Time-dependent density functional theory calculations indicate that the different possible intermediates have very similar absorption spectra, making the unambiguous assignment of the experimentally observed transient absorption of 500 nm to a given species difficult.

Introduction

The cycloaddition of olefins with similar electron density is in most cases fairly slow. One effective way to accelerate these reactions is the use of electron transfer catalysis (ETC), where one of the reaction partners is converted into a radical ion (most commonly a radical cation) through single electron transfer. While the radical cation [4 + 2] cycloaddition has found the most widespread use in synthetic organic chemistry,¹ the ETC [2 + 2] cycloaddition and the analogous cycloreversion is arguably more versatile. Because the corresponding thermal reaction is symmetry-forbidden by Woodward–Hoffmann rules, the photochemical, thermal, and ETC reactions are complementary to each other. This fact was exploited in areas as diverse as solar energy storage² and DNA repair.³

The ETC dimerization of electron-rich styrenes, shown in Scheme 1, has been the most thoroughly investigated ETC

[2 + 2] cycloaddition for a number of reasons. As will be discussed in more detail below, the mechanism of the reaction raises a number of interesting questions and has been very influential in shaping many of the concepts in radical ion chemistry.⁴ The reaction is also important for a number of practical considerations. Styrene radical cations, formed by oxidation by air oxygen⁵ and in heterogeneous systems,⁶ are thought to be involved in the polymerization of styrenes.⁷ This often undesired reaction could lead to practical problems in

(2) (a) Gassman, P. G.; Hershberger, J. W. *J. Org. Chem.* **1987**, *52*, 1337–1339. (b) Wang, X. S.; Zhang, B. W.; Cao, Y. *J. Photochem. Photobiol. A: Chemistry* **1996**, *96*, 193–198.

(3) (a) Sancar, A. *Chem. Rev.* **2003**, *103*, 2203–2237. (b) Harrison, C. B.; O'Neil, L. L.; Wiest, O. *J. Phys. Chem. A* **2005**, *109*, 7001–7012.

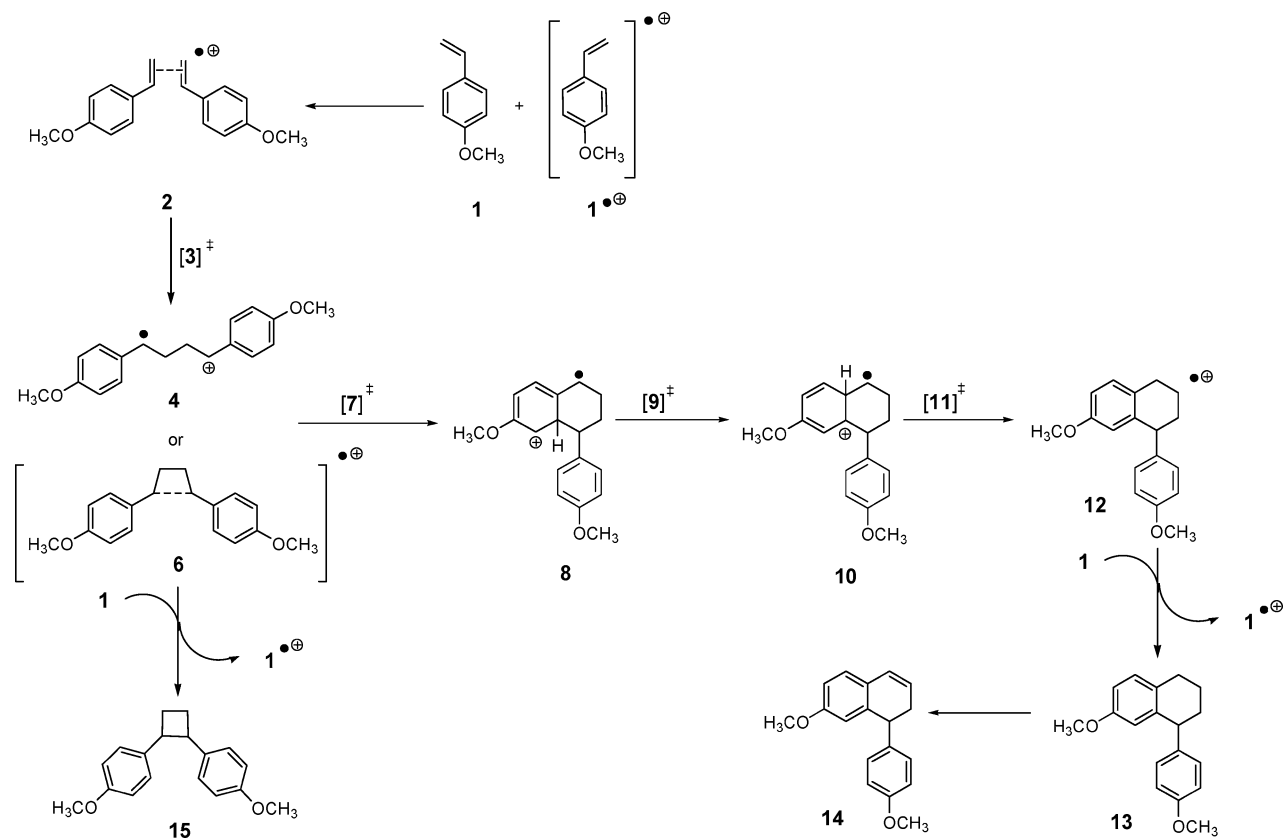
(4) Ledwith, A. *Acc. Chem. Res.* **1972**, *5*, 133–139.

(5) (a) Kojima, M.; Sakuragi, H.; Tokumaru, K. *Bull. Chem. Soc. Jpn.* **1989**, *62*, 3863–3868. (b) Kojima, M.; Sakuragi, H.; Tokumaru, K. *Tetrahedron Lett.* **1981**, *22*, 2889–2892.

(6) (a) Matsubara, C.; Kojima, M. *Tetrahedron Lett.* **1999**, *40*, 3439–3442. (b) Brancalion, L.; Brousmiche, D.; Rao, V. J.; Johnston, L. J.; Ramamurthy, V. *J. Am. Chem. Soc.* **1998**, *120*, 4926–4933.

(1) For example: Rössler, U.; Blechert, S. *Tetrahedron Lett.* **1999**, *40*, 7075–7078. (b) Harichian, B.; Bauld, N. L. *J. Am. Chem. Soc.* **1989**, *111*, 1826–1828.

SCHEME 1. Electron-Transfer-Mediated Dimerization of 4-Methoxystyrene



production facilities and is therefore of great commercial significance. Finally, the products of the reaction are structurally related to several members of the lignane and neolignane family of natural products that have interesting anti-inflammatory and antiviral properties.⁸ It has been proposed that ETC could play a role in the biosynthesis of these compounds.⁹ However, attempts to use ETC for the synthesis of the neolignans only led to yields of less than 20% after extended reaction times.¹⁰ It is therefore clear that systematic improvements of the ETC dimerizations will require a better understanding of the mechanism and the effects controlling them.

The major reaction pathways are summarized in Scheme 1. After one-electron oxidation of **1** by any of a large number of one-electron oxidants and formation of the initial ion–molecule complex **2**, two pathways that differ in the two possible structures for the intermediate have been proposed. Mattes et al.¹¹ suggested a stepwise pathway involving the acyclic tetramethylene radical cation intermediate **4** in analogy to the classic styrene dimerization mechanism proposed by Flory.¹² In contrast, Bauld et al. and Schepp et al.¹³ as well as Lewis et

al.¹⁴ proposed a concerted, nonsynchronous [2 + 1] cycloaddition leading to the long-bond intermediate **6**. Bauld and Pabon proposed the long-bond intermediate based upon the stereospecificity of the reaction, which maintains the geometry of the double bond in substituted styrenes, and MNDO calculations that indicated the intermediate was an energy minimum and that the length of the newly formed C–C bond between the benzylic carbons was 1.92 Å. Further evidence for the long-bond intermediate, provided by Schepp et al., was the observation of a transient species in a photoinduced electron transfer study of the dimerization reaction using laser irradiation. As the absorption of the 4-methoxystyrene decayed, a new absorption at 500 nm was observed which was attributed by exclusion to the hexatriene radical cation **8**, even though it was previously assigned to the acyclic intermediate **4**.¹⁵ Further kinetic studies

(7) (a) Gotoh, T.; Yamamoto, M.; Nishijima, Y. *Polym. Bull. (Berlin)* **1980**, *2*, 357–362. (b) Hayashi, K.; Pepper, D. C. *Polym. J.* **1976**, *8*, 1–9. Compare also c) Bauld, N. L.; Gao, D. *Polym. Int.* **2000**, *49*, 253–259.

(8) E. g.: (a) Kikuchi, T.; Kadota, S.; Yanada, K.; Tanaka, K.; Watanabe, K.; Yoshizaki, M.; Yokoi T.; Shingu, T. *Chem. Pharm. Bull.* **1983**, *31*, 1112–1114. (b) Kobayashi, S.; Inaba, K.; Kimura, I.; Kimura, M. *Biol. Pharm. Bull.* **1998**, *21*, 346–349.

(9) Rodriguez-Evora, Y.; Schepp, N. P. *Org. Biomol. Chem.* **2005**, *3*, 4444–4449.

(10) (a) Marshall Wilson, E.; Dietz, J. G.; Shepherd, T. A.; Ho, D. M.; Schnapp, K. A.; Elder, R. C.; Watkins, J. W.; Geraci, L. S.; Campana, C. F. *J. Am. Chem. Soc.* **1989**, *111*, 1749–1754. (b) Kadota, S.; Tsubono, K.; Makino, K.; Takeshita, M.; Kikuchi, T. *Tetrahedron Lett.* **1987**, *28*, 2857–2860

(11) (a) Mattes, S. L.; Farid, S. *J. Am. Chem. Soc.* **1986**, *108*, 7356–7361. (b) Mattes, S. L.; Farid, S. *Org. Photochem.* **1983**, *6*, 233–326. (c) Mattes, S. L.; Farid, S. *J. Am. Chem. Soc.* **1983**, *105*, 1386–1387. (d) Mattes, S. L.; Farid, S. *J. Am. Chem. Soc.* **1982**, *104*, 1454–1456. See also: (e) Neunteufel, R. A.; Arnold, D. A. *J. Am. Chem. Soc.* **1973**, *95*, 4080–4081.

(12) (a) Flory, P. J. *J. Am. Chem. Soc.* **1937**, *59*, 241–253. For a detailed discussion of the mechanistic possibilities, compare: (b) Pryor, W. A.; Lasswell, L. D. *Adv. Free-Radical Chem* **1975**, *5*, 27–99.

(13) (a) Bauld, N. L.; Pabon, R. *J. Am. Chem. Soc.* **1985**, *105*, 633–634. (b) Schepp, N. P.; Johnston, L. J. *J. Am. Chem. Soc.* **1994**, *116*, 6985–6903. (c) Bauld, N. L. *Tetrahedron* **1989**, *45*, 5307–5363. (d) Schepp, N. P.; Johnston, L. J. *J. Am. Chem. Soc.* **1996**, *118*, 2872–2881. (e) Schepp, N. P.; Shukla, D.; Sarker, H.; Bauld, N. L. *J. Am. Chem. Soc.* **1997**, *119*, 10325–10334. (f) Johnston, L. J.; Schepp, N. P. In: *Advances in Electron-Transfer Chemistry Vol.6*; Mariano, P. S., Ed.; JAI Press: New York 1996, 41–102.

(14) Lewis, F. D.; Kojima, M. *J. Am. Chem. Soc.* **1988**, *110*, 8664–8670.

(15) Tojo, S.; Toki, S.; Takamuku, S. *J. Org. Chem.* **1991**, *56*, 6240–6243.

by Schepp et al. concluded that the rate determining step in the formation of **8** was the cleavage of the long-bond intermediate.^{13b}

Both mechanistic proposals explain the experimental finding that the [2 + 2] product **15** dominates under conditions in which the concentration of styrene is high and for less electron-rich dienes. The [4 + 2] pathway that leads to the tetrahydronaphthalene product **13** is favored by lower styrene concentrations or electron-rich dienes. The tetrahydronaphthalene products are usually oxidized further under the reaction conditions to give the major dihydronaphthalene product **14**. It can also be formed directly from **8** through deprotonation of the radical cation to regain aromaticity, followed by a second one-electron oxidation of the radical and deprotonation of the cation to give **14** without the involvement of **13**. At high styrene concentrations, the radical cation of the [2 + 2] product **6** is quickly reduced by a neutral styrene to give the neutral cyclobutane product **15** and the styrene radical cation **1⁺**. At lower styrene concentrations the radical cation intermediate has time to rearrange to the more stable [4 + 2] product **12**, which is then reduced by a neutral styrene to give **13** and the styrene radical cation **1⁺**. The product ratio of **14** and **15** can therefore be thought of as a measure of the lifetime of the radical cations **4** or **6**. It should be pointed out that the conservation of the stereochemistry of the double bonds does not necessarily imply a concerted mechanism as long as ring closure of **4** is faster than stereochemical scrambling. Experimental studies alone are therefore unlikely to provide the necessary detail in studying this reaction.

Electronic structure calculations have been able to provide detailed insights into the mechanism of radical ion reactions. Surprisingly, little work at high-levels of theory has been published on the dimerization of electron-rich styrenes, despite their importance in the field of radical ion chemistry discussed above. Earlier computational studies of the parent ETC [2 + 2] cycloaddition of ethylene have indicated that the acyclic tetramethylene radical cation is not a minimum on the C₄H₈⁺ potential energy hypersurface and is not involved in either the cycloaddition of ethylene and ethylene radical cation or the cycloreversion of cyclobutane radical cation.^{16,17} The addition of substituents to the system, such as phenyl rings, may stabilize the acyclic intermediate. The two postulated intermediates, the long-bond intermediate formed by concerted cycloaddition and the acyclic structure, are interconvertible through rotation about the central C₂–C₃ bond. Just as with so many other cycloadditions, the detailed mechanism therefore rests on the stability of the acyclic intermediate, which will be strongly influenced by substituent and solvent effects. These effects are difficult to deconvolute experimentally because polar solvents will typically also be good nucleophiles and trap the radical ion intermediate.¹⁸

Calculations performed by Bauld and Pabon indicated that the long-bond intermediate is the key intermediate in the dimerization reaction and was therefore instrumental in formulating this mechanistic hypothesis.^{13a} However, these calculations were performed using the MNDO semiempirical method. There are numerous reports that support a bias of semiempirical methods toward localized structures due to the neglect of overlap.¹⁹ Semiempirical methods are also known to overestimate the stability of structures in which steric repulsion is of concern, such as cyclobutanes.²⁰ The results of a recent high-

level study of the thermal styrene dimerization involving biradical species,²¹ which are often thought to be analogous to the corresponding radical cations,²² suggest that the identification of the long-bond intermediate rather than the acyclic intermediate may be a consequence of the bias associated with semiempirical calculations.

Here, we report the results of the first high-level computational study of this prototypical ETC cycloaddition to dissect the competing [2 + 2] and [4 + 2] pathways using the B3LYP hybrid DFT method, which is known to give accurate results for this and many other radical cationic reactions.^{16,17} We will first discuss the unimolecular pathways for the formation of the [2 + 2] and [4 + 2] products, followed by a discussion of how the competition between the two pathways is influenced by solvent effects. Finally, we will address the assignment of the short-lived species with an absorption band at 500 nm that was identified by Johnston and Toji.

Computational Methodology

All calculations were performed using the Gaussian 03 series of programs.²³ The gas-phase structures were fully optimized at the B3LYP/6-31G* level of theory. All energies reported are in kcal/mol and were corrected for zero-point vibrational energies at the same level of theory. The frequency calculations were also used to determine whether a structure was an energy minimum (no imaginary frequencies) or a transition structure (one imaginary frequency). For the pathway that leads from **8** to **14**, only the unimolecular pathway was considered. The bimolecular pathway would involve deprotonation of **8** to form the radical, electron transfer to form the cation, and deprotonation to form **14**. While in the condensed phase, this bimolecular pathway is likely to be lower in energy than the unimolecular pathway; the deprotonation–electron transfer–deprotonation sequence cannot be treated accurately with the methodology used here. However, these steps can be reasonably assumed to be fast and occur after the product-determining step, which is generally considered^{11,13,14} to be governed by the relative rates of back-electron-transfer and rearrangement.

When using the CPCM solvation model ($\epsilon = 81$) the energies reported are from single-point analysis at the 6-31G* level of the optimized geometries from the gas-phase calculations.²⁴ Validation studies on select structures along the reaction pathways indicate that the differences between single point energies and those resulting from full optimizations were between 0 and 0.3 kcal/mol. The small difference in energies for the fully optimized structures and the single points indicates that single point calculations are viable for the reaction of interest.

Time-dependent density functional theory (TD-DFT) calculations were carried out at the B3LYP/6-311+G** level of theory.²⁵ For

(16) (a) Jungwirth, P.; Carsky, P.; Bally, T. *J. Am. Chem. Soc.* **1993**, *115*, 5776–5782 (b) Jungwirth, P.; Carsky, P.; Bally, T. *J. Am. Chem. Soc.* **1993**, *115*, 5783–5789.

(17) Wiest, O. *J. Phys. Chem. A* **1999**, *103*, 7907–7911.

(18) Weng, H.; Roth, H. *J. Org. Chem.* **1995**, *60*, 4136–4145.

(19) (a) Caramella, P.; Houk, K. N.; Domelsmith, L. N. *J. Am. Chem. Soc.* **1977**, *99*, 4511–4514. (b) Brown, A.; Dewar, M. J. S.; Schoeller, W. *J. Am. Chem. Soc.* **1977**, *99*, 5096–5097. (c) Houk, K. N.; González, J.; Li, Y. *Acc. Chem. Res.* **1995**, *28*, 81–90. (d) Anh, N. T.; Frison, G.; Solladié-Cavallo, A.; Metzner, P. *Tetrahedron* **1998**, *54*, 12841–12852.

(20) Clark, T. *Handbook of Computational Chemistry*; Wiley & Sons: New York, 1985.

(21) (a) Khuong, K. S.; Jones, W. H.; Pryor, W. A.; Houk, K. N. *J. Am. Chem. Soc.* **2005**, *127*, 1265–1277. (b) Northrup, B. H.; Houk, K. N. *J. Org. Chem.* **2006**, *71*, 3–13.

(22) (a) Wiest, O.; Oxgaard, J.; Saettel, N. *J. Adv. Phys. Org. Chem.* **2003**, *39*, 87–109. (b) Donoghue, P. J.; Wiest, O. *Chem. Eur. J.* **2006**, *12*, 7018–7026.

(23) Frisch, M. J.; et al. *Gaussian 03*, Revision C.02; Gaussian, Inc.: Wallingford CT, 2004.

(24) (a) Miertus, S.; Scrocco, E.; Tomasi, E. *Chem. Phys.* **1981**, *55*, 117–129. (b) Barone, V.; Cossi, M. *J. Chem. Phys. A* **1998**, *102*, 1995–2001. (c) Cossi, M.; Rega, N.; Scalmani, G.; Barone, V. *J. Comput. Chem.* **2003**, *24*, 669–681.

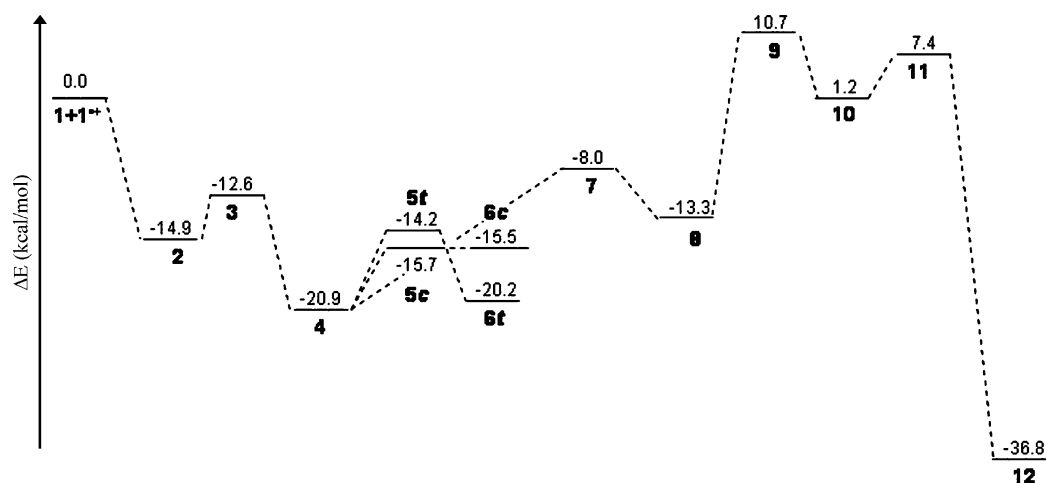


FIGURE 1. Reaction diagram for the gas-phase electron-transfer-mediated dimerization of 4-methoxystyrene computed at the B3LYP/6-31G* level of theory.

a recent review of TD-DFT methods, see ref 25d. This method has also been applied to the calculation of the electronic excited states of radical cations with one example reporting the standard deviation between experimental and computational to be less than 0.3 eV for polycyclic aromatic hydrocarbon radical ions.²⁶ The TD-DFT calculations were also performed using nonequilibrium solvation as provided by the PCM model. In the development of this method, it was noted that PCM performs better than CPCM for polar solvents.²⁷

Results and Discussion

As shown in Scheme 1, ET and dimerization of **1** leads to two reaction manifolds, giving the cyclobutane and tetrahydronaphthalene products, respectively. Although cage processes cannot be completely excluded, these intermediates are generally treated as free radical cations based on the finding that there are few differences observed between the reactivity of neutral acceptors, which could form caged ion pairs, and cationic acceptors,²⁸ that do not. The energy diagram for the pathways leading to the formation of both the cyclobutane and tetrahydronaphthalene products in the gas phase is shown in Figure 1.

The first step of the reaction is the formation of an ion–molecule complex between the neutral and radical cationic species, **2**, which is favorable in the gas phase by 14.9 kcal/mol. There is a small barrier of 2.3 kcal/mol for the formation of the acyclic intermediate **4**. The first branching point between the cyclobutane and the tetrahydronaphthalene pathways occurs at the acyclic intermediate. This diversion could also occur at the *trans* isomer of the long-bond intermediate **6t** through a [1,3] sigmatropic shift, as will be discussed below.

From the acyclic intermediate **4**, there is an activation energy of 12.9 kcal/mol to the transition state, **7**, in the first step of the [4 + 2] pathway in the gas phase. The product of this step is the hexatriene radical cation **8**, which is 7.6 kcal/mol higher in

energy than the acyclic intermediate **4**. In the unimolecular pathway discussed here, **8** can then undergo a [1,2] hydrogen shift to produce **10** with an activation energy of 24 kcal/mol and a reaction energy of +14.5 kcal/mol. Another hydrogen shift produces **12**, which is much more stable than **10**, as reflected in the change in energy of −38.0 kcal/mol. The large activation energies and energy changes for the tetrahydronaphthalene pathway make it a kinetically less favorable pathway than the cyclobutane pathway. The last step of the [4 + 2] pathway is very thermodynamically favorable and drives the otherwise unfavorable pathway. Since the cyclobutane product can be converted to the hexatriene radical cation **8** before it is reduced to the neutral form, the equilibrium can be established and the more favorable product, **12**, can be formed in the gas phase. In solution, the bimolecular pathway discussed earlier can lead directly to the low-energy structure **14**.

The hexatriene radical cation **8** could also be produced via a vinylcyclobutane rearrangement of **6**. The transition structure for this reaction was located and was found to be essentially identical to **7**. There was a small energy difference between **7** and the transition structure for a vinylcyclobutane rearrangement, −0.8 kcal/mol, which can be attributed to the fact that the two transition states are cyclohexane ring-flip isomers. The coordinates for this structure are given in the Supporting Information.

The alternative cyclobutane pathway can produce either *cis*- or *trans*-1,2-bis(4-methoxyphenyl)cyclobutane (**6c** and **6t**) via **4**, i.e., in a stepwise fashion. Unlike the prediction from the MNDO calculations, we were unable to locate a concerted pathway from **2** to **6**. While the activation energy for the production of the *cis* isomer **6c** is 5.2 kcal/mol lower than that for the *trans* isomer of 6.7 kcal/mol, the *trans* isomer is predicted to be more thermodynamically stable. This is in agreement with the fact that the *trans* isomer is the only observed product for the cyclobutane pathway, as reported by Schepp et al.^{13b} The *cis* isomer is less thermodynamically stable than the *trans* isomer due to the increased steric strain and crowding of the *p*-methoxyphenyl groups on the cyclobutane ring. Interestingly, these effects are stronger than the stabilization that could be achieved by π -stacking of the aryl groups in **6c**, possibly because the delocalization of spin and charge into the rings leads actually to a repulsive interaction. It is also known experimentally that **6c** can be converted to **14** or **6t** under ETC conditions. This is readily apparent from the results shown in Figure 1, which show

(25) (a) Bauernschmitt, R.; Ahlrichs, R. *Chem. Phys. Lett.* **1996**, *256*, 454–464. (b) Stratmann, R. E.; Scuseria, G. E.; Frisch, M. J. *J. Chem. Phys.* **1998**, *109*, 8218–8224. (c) Casida, M. E.; Jamorski, C.; Casida, K. C.; Salahub, D. R. *J. Chem. Phys.* **1998**, *108*, 4439–4449. (d) Burke, K.; Werschnik, J.; Gross, E. K. U. *J. Chem. Phys.* **2005**, *123*, 62206–62215.

(26) Hirata, S.; Head-Gordon, M.; Szczepanski, J.; Vala, M. *J. Phys. Chem. A* **2003**, *107*, 4940–4951.

(27) Cossi, M.; Barone, V. *J. Chem. Phys.* **2001**, *115*, 4708–4717.

(28) Meyer, S.; Koch, R.; Metzger, J. O. *Angew. Chem., Intl. Ed.* **2003**, *42*, 4700–4703.

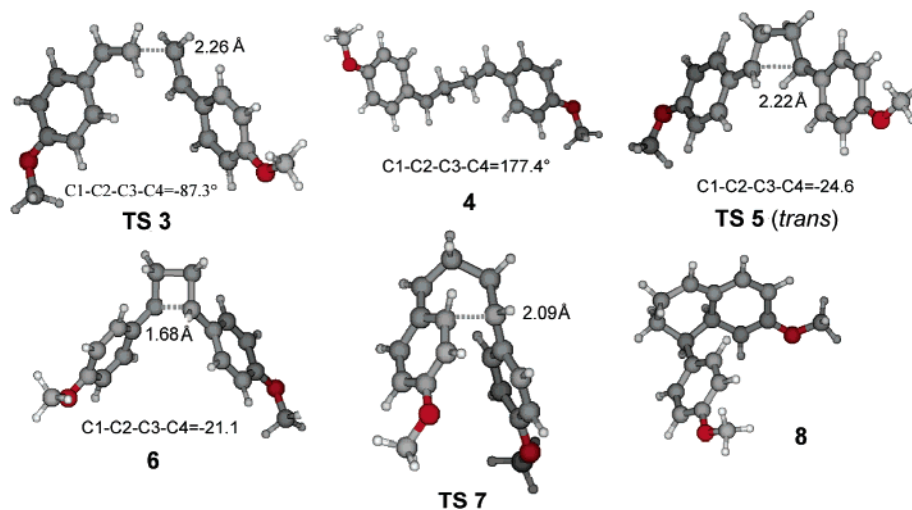


FIGURE 2. Optimized structures (B3LYP/6-31G*) of **TS 3**, acyclic intermediate **4**, **TS 5 (trans)**, long-bond intermediate **6**, **TS 7**, and hexatriene radical cation **8**.

that the pathway leading from **6c** to **4** is essentially barrierless and 5.4 kcal/mol downhill in the gas phase. The ΔE for the reaction is 0.2 kcal/mol greater than the ΔE^\ddagger for the reaction due to the addition of the zero-point energy to the computed SCF energies. In contrast, **4** and **6t** are essentially isoenergetic and will interconvert rapidly via **5t**. The optimized structures for the long-bond and acyclic intermediates, the hexatriene radical cation, and the structures of the transition states that lead to each are shown in Figure 2.

As was the case in a number of other systems,²² the structures shown in Figure 2 are similar to the ones obtained in a computational study of the corresponding neutral reaction of styrenes involving biradicals. In contrast to the results from the MNDO and transient absorption studies, the transition structure **TS 3** has a dihedral angle of 87.3° around the central C₂–C₃ bond. Therefore, no interaction between the benzylic carbons is expected. The key intermediate in the dimerization reaction^{13a} identified by Bauld and Pabon was a long-bond intermediate with a bond distance of 1.92 Å. These calculations were performed using a semiempirical method, MNDO, which has been shown to prefer asynchronous structures due to the neglect of differential diatomic overlap.^{19a} Examples of the preference of semiempirical methods to asynchronous structures can be found in Dewar's investigation of the Cope rearrangement and Houk's investigation of the Diels–Alder reaction, among others.¹⁹ The neglect of overlap in MNDO calculations also biases toward localization of spin and charge, which may explain why the C₁–C₄ bond distance in the structure calculated by Bauld and Pabon, 1.92 Å, is much greater than the distances in our structures, 1.72 and 1.68 Å for **6c** and **6t**, respectively. Semiempirical methods are also known to overestimate the stability of structures in which steric repulsion is of concern, such as cyclobutanes.^{19d} The identification of the long-bond intermediate, and not the acyclic intermediate, by Bauld and Pabon may be a consequence of the problems associated with semiempirical calculations on reactions of this type. These differences raised the question of whether other conformations of **4** would be structurally more similar to the structure described by Bauld. Therefore, we studied the interconversion of **4** and **6** by rotation around the C₁–C₂ and C₂–C₃ bonds, as shown in Figure 3. The corresponding dihedral angles were scanned with a stepsize of 15° for a total of 23 steps.

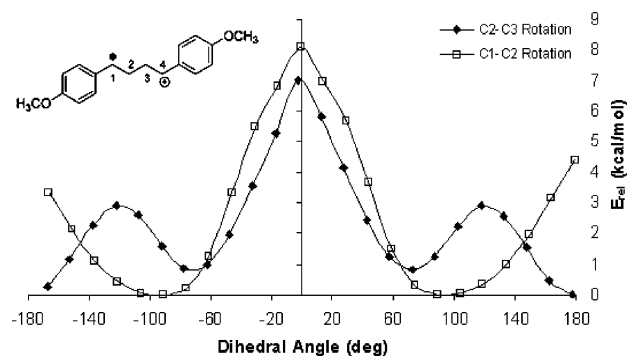


FIGURE 3. Potential energy vs dihedral angle for rotation around the C₁–C₂ (□) and C₂–C₃ bonds (◆).

As expected, the extended structure that corresponds to the acyclic intermediate, with a dihedral angle of 177.4°, is the most stable. The dihedral angles of **6c** and **6t** are 20.4° and –21.1°, respectively. The corresponding relative energies for the structures calculated in the dihedral scan that correspond to those angles are ~5 kcal/mol. The reaction energies for the formation of **6c** and **6t** from the acyclic intermediate are 5.4 and 0.7 kcal/mol, respectively. The difference in the energy between optimized **6c** and **6t** and the dihedral scan structures indicates that there are differences in the calculated structures. This energy difference is due to the difference in the C₁–C₄ bond distance. The C₁–C₄ distance in the dihedral angle rotation structures is ~3 Å for both the *cis* and *trans* isomers. The same distance in the optimized structures of **6c** and **6t** are 1.74 and 1.68 Å, respectively, indicating again the repulsive nature of the aryl interaction in **6c**. These structures of **6** and **4** are then connected through **TS 5**, shown in Figure 2, where the lengths of the forming bond is 2.22 Å. These results support the idea that the interconversion between the long-bond and acyclic intermediates by rotation around the C₂–C₃ bond is, with an activation energy of 2.9 kcal/mol, quite facile and an important part of this reaction.

These results also explain the experimentally observed stereospecificity¹³ of the reaction. As can be seen in Figure 3, the barriers for rotation around the C₂–C₃ bond are higher than the barriers for ring closure summarized in Figures 1 and 5.

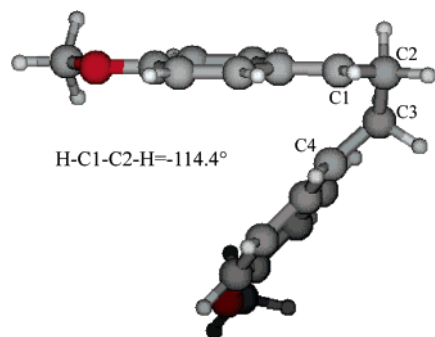


FIGURE 4. Structure of acyclic intermediate **4** with $C_1-C_2-C_3-C_4 = -2.6^\circ$.

The stereoselectivity may therefore result from rapid ring closure and does necessarily implicate the long-bond intermediate **6**.

The relatively high barriers for rotation around the C_1-C_2 bond shown in Figure 3 are in marked contrast to the results for the biradical species. Computational studies of the thermal polymerization of styrene show that the 1,4-diradical produced in the first step of the reaction can adopt many conformations that are all essentially isoenergetic.^{21a} Different conformations of the 1,4-diradical can undergo further reaction to form either a diphenylcyclobutane or a neutral hexatriene structure that is analogous to the hexatriene radical cation **8**. This is also observed for the study of the vinylcyclobutane–cyclohexene rearrangement.^{21b} The diradical intermediate exists on a flat surface, which allows rapid interconversion of conformers of this structure, whereas the radical cation is configurationally stable. Analysis of the high-energy structures from Figure 3 provides insights into the origin of these marked differences. Figure 4 shows the structure of acyclic intermediate **4** with $C_1-C_2-C_3-C_4$ dihedral angle set to -2.6° .

The reason for the high energy of this structure is readily apparent from the fact that the $H-C-C-H$ angle required for hyperconjugation is 90° . As shown in Figure 4, the $H-C_1-C_2-H$ dihedral angle is -114.4° , resulting in poor overlap. The $H-C_4-C_3-H$ dihedral angle is 86.4° , allowing for overlap of the empty p-orbital with the σ of the $C-H$ bonds on C_3 . A rotation about the C_1-C_2 bond would allow hyperconjugation between the radical and the C_2 hydrogens, but it would also place the two ortho hydrogens on the aryl rings in close contact. Therefore, only one of the two centers can be stabilized by hyperconjugation. This effect is even stronger for rotation around the C_1-C_2 bond, which directly disrupts hyperconjugation. This effect is expected to be much stronger in the radical cation than in the radical, because the interaction of the empty orbital with the filled σ -orbital of the $C-H$ will be stronger than that of a singly occupied p-orbital in the radical. To the best of our knowledge, this conformational effect based on differences in hyperconjugation of radicals and cations has not yet been described for distonic radical cations. Future studies will have to determine how general this effect is and how relevant it is for the frequently observed high selectivity of radical cation reactions.

Next, we studied how the reaction pathway will be influenced by solvation using a CPCM model. The use of an implicit solvent as provided by the CPCM solvent model allows evaluations of the solvent effects on a reaction when the inclusion of an explicit solvent is not feasible. The energy

diagram for the production of both the cyclobutane and tetrahydronaphthalene products in the condensed phase is shown in Figure 5.

As in the gas-phase reaction, the condensed phase reaction begins with the formation of the complex **2** between the neutral and radical cationic 4-methoxystyrenes. The acyclic intermediate is then formed with a ΔE^\ddagger of 1.0 kcal/mol and a ΔE of 6.6 kcal/mol. The acyclic intermediate **4** and *trans*-1,2-bis(4-methoxyphenyl)cyclobutane (**6t**) are essentially isoenergetic. The formation of the *cis* isomer of the long-bond intermediate **6c** is barrierless, as was also observed in the gas-phase calculations. From **4** there is an activation energy of 10.3 kcal/mol to produce **7**. The product of this step of the pathway, **8**, is 2.4 kcal/mol higher in energy than **4**. The hexatriene radical cation **8** then undergoes a hydrogen shift to produce **10** with a ΔE of 14.8 kcal/mol. The final step of the $[4+2]$ pathway is the formation of **12**, which is the thermodynamic driving force for the pathway as reflected in the ΔE of -32.3 kcal/mol.

The condensed phase calculations were performed in order to evaluate the stabilization provided by a polar solvent to the $[4+2]$ pathway. The energy difference between the two pathways in the gas phase is 24.9 kcal/mol. In the condensed phase, this difference drops to 18.6 kcal/mol, making the tetrahydronaphthalene pathway more thermodynamically feasible. The decrease in the energetic cost of the tetrahydronaphthalene pathway can be attributed to the formation of the hexatriene radical cation **8** from the acyclic intermediate **4**. The activation energy of that step is 12.9 kcal/mol in the gas phase but only 10.3 kcal/mol in the condensed phase. The ΔE for the reaction is 7.6 kcal/mol in the gas phase, but in the condensed phase this drops to 2.4 kcal/mol, a difference of 5.2 kcal/mol. The hexatriene radical cation **8** benefits from the stabilization provided by water more than the acyclic intermediate **4** because of the poor resonance stabilization of the charge and spin.

Finally, we addressed the assignment of the transient absorption at 500 nm to the hexatriene radical cation **8**. A comparison of the experimentally observed absorption wavelength to that of the calculated reaction intermediates, specifically the acyclic intermediate **4**, the long-bond intermediate **6**, and the hexatriene radical cation **8**, was performed using TD-DFT methods in the gas phase and PCM.²⁵ The excitations that are relevant for the following discussion are included in Table 1. For a listing of all of the excitations predicted by the TD-DFT calculations, see the Supporting Information.

Previous work by Tojo et al. implicated the acyclic intermediate **4** in the dimerization reaction based upon pulse radiolysis studies.¹⁵ After irradiation of 4-methoxystyrene **1**, the radical cation **1**^{•+} was observed at 600 nm along with a transient absorption at 505 nm. The decay of the 600-nm band led to simultaneous formation of the 505-nm band, leading the authors to the conclusion that the 505-nm band corresponded to a dimer of 4-methoxystyrene. Further pulse radiolysis studies showed that the efficiency of the formation of the 505-nm band was greater for **6c**, the more highly strained isomer, than for **6t**. This led the authors' assignment of the 505-nm band to the acyclic intermediate **4**.

The transient species with the absorption at 500 nm was also observed in 10-ns laser flash studies.^{13b} It was proposed that the absorption spectrum of the acyclic intermediate would, in analogy to the isolated chromophores, appear in the 300–340-nm region. The kinetic data for the ring cleavage of the cyclobutane product showed that the decay of the 500-nm band

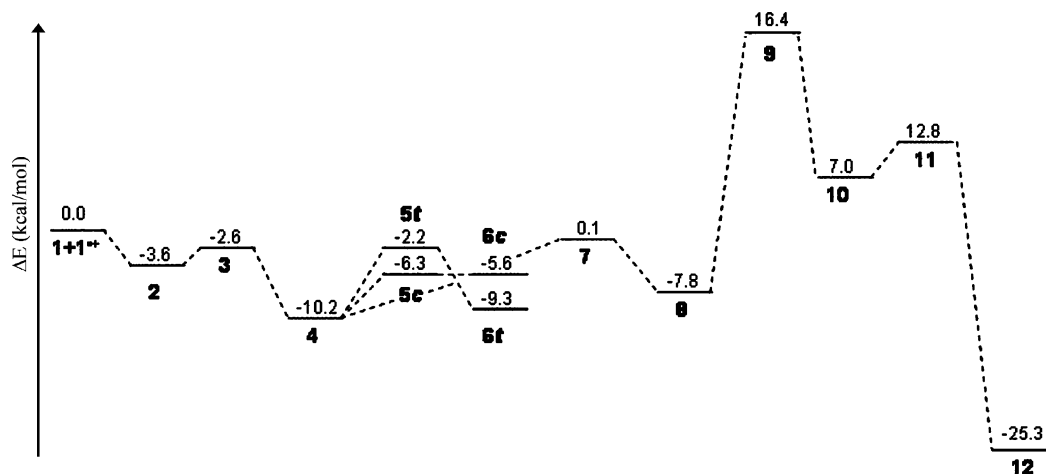


FIGURE 5. Reaction diagram for the condensed phase electron-transfer mediated dimerization of 4-methoxystyrene computed at the CPCM//B3LYP/6-31G* ($\epsilon = 81$) level of theory.

TABLE 1. Calculated (TD-DFT) Electronic Excitations of the Selected Reaction Intermediates

compd	gas phase		PCM ($\epsilon = 36.6$)	
	absorption wavelength (nm)	transition dipole	absorption wavelength (nm)	transition dipole
4	499.9	0.11	479.8	0.11
6t	498.0	0.06	508.3	0.07
6c	506.7	0.10	515.9	0.13
8	529.1	0.02	487.9	0.01

did not precede the observation of the 600-nm band, as would be expected for both the acyclic and long-bond intermediates. In addition, the 4-methoxystyrene concentration has no effect on the decay of the 500-nm band, as would be expected for the long-bond intermediate. The 500-nm transient was therefore attributed to the hexatriene radical cation **8** by exclusion and rationalized by the observation that other similar hexatriene systems absorb at ~ 430 nm, and the addition of methoxy substituents to the phenyl rings would shift the absorption to a higher wavelength. It was concluded that the rate of the cleavage of the cyclobutane radical cation would be too fast for the reduction by neutral styrene to compete if the acyclic intermediate was included. Therefore, the mechanism proposed as a result of this work does not include an acyclic intermediate.

On the basis of our calculations, the rates for interconversion of **4** and **6** are on the order of 10^7 – 10^{10} s^{-1} , while the formation of **8** from **6t** is predicted to be $\sim 10^6$ s^{-1} in solution, which is in the same time scale as the laser pulse used in the experiments. The TD-DFT calculations indicate that there are absorptions close to 500 nm for both the acyclic intermediate **4** and the long-bond intermediates **6c** and **6t** in both the gas and condensed phases. Although there are absorptions in the 340–390-nm range for either species, the intensity of these absorptions is less than or equal to the 500-nm band. In addition, the calculated absorption wavelength of the hexatriene radical cation **8** is 529.1 nm in the gas phase and 487.9 nm in the condensed phase. The results of the TD-DFT calculations for all of the intermediates in question are therefore all in the same range. On the basis of the results of the TD-DFT calculations, it appears that the transient absorption at 500 nm cannot be reliably assigned to one of the intermediates because there is very little difference in the electronic structure of their chromophores. In addition, the calculations presented here indicate that the long-bond and

acyclic intermediates, **6t** and **4**, can rapidly interconvert due to the small barrier and can therefore not be considered different species on the time scale of the laser flash experiment but rather as a mixture of the two.

Conclusions

The electron-transfer-mediated dimerization of 4-methoxystyrene has been proposed to proceed via one of two possible mechanisms, a stepwise pathway via an acyclic intermediate or a concerted process leading to a long-bond intermediate. Electronic structure calculations show that the reaction is stepwise and that the acyclic intermediate **4** and the *trans* isomer of the long-bond intermediate **6t** are essentially isoenergetic. The two intermediates can be interconverted by the rotation of a dihedral angle, followed by ring closure with a barrier of 6.7 kcal/mol. While one may think of these two intermediates as separate structures, it would also be valid to consider them as rapidly equilibrating conformers.

From the key intermediate of the reaction, **4**, there are two possible pathways to follow. The [2 + 2] pathway produces a cyclobutane, while the [4 + 2] pathway produces a tetrahydronaphthalene, which is usually oxidized to a dihydronaphthalene under the reaction conditions. Since the [4 + 2] pathway involves poor stabilization of the spin and charge associated with the radical cation, this reaction pathway is in the gas phase significantly higher in energy than the [2 + 2] pathway. The inclusion of a polar solvent, water, without the addition of a nucleophile was performed using the CPCM solvation model. The energy difference between the two pathways was decreased in the condensed phase, with the majority of the energy difference attributable to the formation of the hexatriene radical cation **8**. This indicates that the [4 + 2] pathway was indeed stabilized by a polar solvent. In the condensed phase, the direct deprotonation of **8** is an alternative pathway that circumvents the high-energy steps and leads directly to the thermodynamically stable **14**. The differences between the results of the TD-DFT calculations the results from previous laser flash studies that supported a concerted mechanism can be rationalized by considering the lifetimes of the intermediates involved as well as the fact that they are predicted to have very similar absorption spectra.

These results raise the intriguing possibility that the selectivity of the reaction can be controlled by the solvent beyond the

previously proposed partitioning based on the lifetime of the intermediate radical ions. This would require fairly polar but nonnucleophilic solvents. A good example of this type of solvent would be an ionic liquid, such as those based upon the 1-butyl-3-methylimidazolium cation with BF_4 , $\text{N}(\text{Tf})_2$ or various²⁹ other anions. The ions would stabilize the radical cation without the possibility of nucleophilic attack on the substrate. Further studies, including the exploration of the product distribution of the reaction of various substituted styrenes in nonpolar solvents and ionic liquids, are currently in process in our laboratory.

(29) Compare also: Ciminale, F.; Lopez, L.; Paradiso, V.; Nacci, A. *Tetrahedron* **1996**, *52*, 13971–13980.

Acknowledgment. We gratefully acknowledge financial support of this work by NSF (Grant No. CHE-0415344 to O.W.) and the allocation of computer resources by the Center for Research Computing at the University of Notre Dame. L.L.O. is the recipient of a Schmitt Fellowship by the University of Notre Dame.

Supporting Information Available: Cartesian coordinates of all stationary points reported, their absolute energies in hartrees, and any imaginary frequencies for **1–12**, TD-DFT calculations, and the full author list for ref 23. The absolute energies in hartrees, the relative energies in kcal/mol and selected $\text{C}_1\text{—C}_4$ bond lengths for the dihedral scan are also given. This information is available free of charge via the Internet at <http://pubs.acs.org>.

JO061745B